COMPOSITIONAL AND STRUCTURAL VARIABILITIES OF MG-RICH IRON OXIDE SPINELS FROM TUFFITE[1]

W. N. MUSSEL[2], J. D. FABRIS[2], J. M. D. COEY[3], L. M. A. SANS[4] & M. F. F. LELIS[5]

SUMMARY

Maghemite (γFe_2O_3) from tuffite is exceptionally rich in Mg, relatively to most of those reportedly found in other mafic lithosystems. To investigate in detail the compositional and structural variabilities of this natural magnetic iron oxide, sets of crystals were isolated from samples collected at different positions in a tuffite weathering mantle. These sets of crystal were individually powdered and studied by X-ray diffractometry, Mössbauer spectroscopy, magnetization measurements and chemical analysis. Lattice parameter of the cubic cell (a_0) was found to vary from 0.834(1) to 0.8412(1) nm. Lower a_0-values are characteristic of maghemite whereas higher ones are related to a magnetite precursor. FeO content ranges up to 17 mass % and spontaneous magnetization ranges from 8 to 32 J T^{-1} kg^{-1}. Zero-field room temperature Mössbauer spectra are rather complex, indicating that the hyperfine field distributions due to Fe^{3+} and mixed valence $Fe^{3+/2+}$ overlap. The structural variabilities of the (Mg, Ti)-rich iron oxide spinels is essentially related to the range of chemical composition of its precursor (Mg, Ti)-rich magnetite, and probably to the extent to which it has been oxidized during transformation in soil.

Index terms: magnetization, Mössbauer, magnetic soil.

RESUMO: *VARIABILIDADES COMPOSICIONAL E ESTRUTURAL DE ÓXIDOS DE FERRO RICOS EM Mg DE TUFITO*

A maghemita (γFe_2O_3) de tufito é, excepcionalmente, rica em magnésio, se comparada às comumente encontradas em outros litossistemas máficos. Na tentativa de investigar em detalhes a variabilidades composicional e estrutural desses óxidos naturais de ferro, alguns

[1] Recebido para publicação em setembro de 1998 e aprovado em agosto de 1999.
[2] Professor do Departamento de Química, ICEx, Universidade Federal de Minas Gerais - UFMG. CEP 31270-901 Belo Horizonte (MG).
[3] Professor do Department of Physics, Trinity College, University of Dublin, Dublin 2, Ireland.
[4] Pesquisador da Embrapa Milho e Sorgo. CEP 35701-970 Sete Lagoas (MG).
[5] Professora do Departamento de Química, UFES. CEP 29069-900 Vitória (ES).

conjuntos de cristais foram separados de amostras coletadas a diferentes posições de um manto de intemperismo de tufito. Esses conjuntos de cristais foram, individualmente, estudados por difração de raios-X, espectroscopia Mössbauer, medidas de magnetização e análise química. Da difratometria de raios-X, observou-se que o parâmetro da célula cúbica (a_0) varia de 0,834(1) a 0,8412(1) nm. Os valores mais baixos de a_0 são característicos de maghemita; os mais altos são atribuídos à magnetita, mineral magnético precursor. Os teores de FeO alcançam 17 mass % e os valores de magnetização espontânea variam de 8 a 32 J T^{-1} kg^{-1}. Os espectros Mössbauer, obtidos com a amostra mantida à temperatura do ambiente, na ausência de campo magnético aplicado, são bastante complexos, com indicações de ocorrência de superposição de distribuições de campo hiperfino, devidas ao Fe^{3+} e ao íon de valência mista $Fe^{3+/2+}$. A variabilidade estrutural dos óxidos de ferro, isoestruturais ao espinélio e ricos em Mg e Ti, é, essencialmente, relacionada com os graus variáveis de oxidação do mineral precursor, a magnetita rica em Mg e Ti.

Termos de indexação: magnetização, Mössbauer, solos magnéticos.

INTRODUCTION

A (Mg, Ti)-rich maghemite from tuffite, a mafic rock formed from volcanic ashes from the Alto Paranaíba region, in Minas Gerais, Brazil, was earlier identified (Fabris et al., 1994) and characterized (Fabris et al., 1995). Goulart et al. (1997) have shown evidences of multiple spinel phases in a soil developing on tuffite of that same area, with different chemical compositions and unit cell dimensions determined from the (440)-reflection. One of these phases had a similar composition to the (Mg, Ti)-rich maghemite described by Fabris et al. (1995). It was later suggested that structural iron in the inner phase of some grains of iron rich spinel from tuffite had a ferrous character (Fabris et al., 1997). Whether the structural heterogeneity of such iron oxide spinels is of a wider spatial occurrence than that reported in single-sample studies (Fabris et al., 1997; Goulart et al., 1997) in that system was no clear at that time.

The purpose of this work was to examine iron-rich spinel phases from samples collected at various depths in a weathering mantle of tuffite in the Alto Paranaíba region, to investigate, in more detail, a large number of samples, in an attempt to provide more data allowing to form a broader and more general picture of their compositional and structural variabilities.

EXPERIMENTAL METHODS

The tuffite deposit is approximately 100 m thick, over Bauru sandstone in the Cretaceous Mata da Corda Formation. It is a pyroclastic material derived from a long-extinct volcanic source and covers an area of about 5000 km². The greenish-grey tuffite mantle was exposed in a road-cut of the BR 365 highway, 23.5 km north of Patos de Minas, Minas Gerais, in the Central Plateau of Brazil. It is overlain by a 6 m deep Dusky Red Oxisol, which is strongly magnetic (Carmo et al., 1984; Curi, 1984; Ferreira et al., 1994).

The tuffite is porous and friable. It is easily reduced to a powder composed of micron-sized grains. Five samples were collected at depths of 4, 6, 10, 12 and 14 m from the top of the mantle. The 4 m sample corresponds to the B horizon of the Oxisol; the others are materials from the parent rock. The samples were gently crushed in a non-magnetic steel mortar. The powdered material was left in a teflon beaker with 5 mol L^{-1} NaOH at room temperature for 24 h, under stirring in a magnetic stirrer. The residual solid portions were then washed and black magnetic particles were picked up with a hand magnet. Only the magnetic fractions were kept for further analyses. Submillimeter crystals exhibiting an octahedral habit were then collected from the magnetic separates under a binocular lens. Sets of some tens of crystals were then analyzed for their chemical composition, and by powder X-ray diffractometry, magnetometry and Mössbauer measurements.

Chemical analysis was performed according to standard methods described by Jeffery & Hutchison (1981). The sample materials were brought into solution by grinding about 10-20 mg of crystals and dissolving the powder with hydrochloric acid 1:1. The Fe^{2+} was determined by dissolving separate samples in concentrated HCl in a CO_2 atmosphere. Total Al, Ca, Cr, Fe, Li, Mg, Ni, Si and Ti, and minor elements, namely As, Cu, Hg, K, Mn, Mo, Na and Zn, were analyzed in a Shimadzu plasma emission spectrophotometer model ICPQ-1014. The Ca^{2+} was determined in a Perkin-Elmer absorption spectrophotometer model 3300; Na^+ and K^+ were

determined in a Micronal flame photometer model B262. The averaged compositions in mass % are presented in Table 1. Polished sections of selected crystals, mounted in a Buehler Transoptic powder resin and covered with a thin carbon layer, were probed with a Jeol 733 scanning electron microscope, equipped with an energy-dispersive X-ray spectrometer.

The powder X-ray diffraction (XRD) pattern was obtained with a Siemmens D500 powder diffractometer, using graphite monochromator, CuKa radiation and 0.05° 2θ/min of step scanning under 40 KV at 40 mA of voltage and current, respectively. Silicon was used as an external standard. Optical micropetrographical analyses were performed on polished sections of some crystals, under polarized light.

The spontaneous magnetization was obtained with a compact vibrating sample magnetometer conceived by Cugat et al. (1994). Mössbauer spectra were recorded in a conventional constant acceleration transmission spectrometer and a Co^{57}/Rh source, at room temperature and 80 K. AC-susceptibility was measured with a conventional vibrating Oxford susceptometer, the sample being submitted to varying temperatures from 77 K up to 280 K, under a magnetic field of 1 oersted in a frequency of 3000 Hz.

RESULTS AND DISCUSSION

X-ray measurements

The X-ray patterns (Figure 1) reveal a large structural variabilities of the iron-spinel throughout the mantle, confirming, now in more detail, previously reported evidence of multiple spinel structures in soil developing on tuffite (Goulart et al., 1997), and in its parent material (Fabris et al., 1997). Diagnostic reflections of the spinel phases are split, in the present case, in all samples. No characteristic line due to superstructure is observed for maghemite. Two groups of the cubic cell dimensions can be identified from this data (Figure 1). In one group, with higher unit cell-dimensions, a_0 ranges from 0.8397 nm up to 0.8412 nm; in the other, a_0 ranges from 0.834 nm up to 0.838 nm. Actually, the reported lattice parameter a_0 = 0.8417 nm for the Fe^{2+}-containing soil iron-spinel from Goulart et al. (1997) is significantly higher than the characteristic a_0 = 0.8380(2) nm of the fully oxidized (Mg, Ti)-rich maghemite (Fabris et al., 1995) from the parent tuffite. A further study by Fabris et al. (1997) on a set of crystals of the iron-spinel from this tuffite revealed an Fe^{2+} content of up to 13 mass %. The powder X-ray analysis also indicated that two spinel phases coexist in the sample: one with higher

Table 1. Chemical composition of a set of crystals according to the sampling depth in the weathering mantle. The numbers in parentheses are uncertainties over the last significant digit estimated as mean standard deviations of independent determinations from three aliquots

Chemical composition	Sampling depth (m)				
	4	6	10	12	14
			mass %		
Fe_2O_3	57 (2)	62 (1)	52 (2)	52 (2)	55 (4)
FeO	7.9 (7)	11.28 (9)	16.9 (7)	12.9 (4)	15.5 (9)
TiO_2	13 (4)	12 (2)	14.3 (8)	12.7 (4)	12.5 (5)
MgO	6.5 (3)	6 (3)	9 (2)	8 (2)	4.7 (3)
Al_2O_3	2.4 (4)	3.5 (6)	2 (2)	3 (1)	6 (3)
CaO	2.5 (2)	0.9 (2)	1.1 (4)	0.81 (9)	1.3 (4)
K_2O	(-)	0.8 (2)	(-)	(-)	0.5 (5)
SiO_2	4.1 (2)	0.6 (2)	0.36 (3)	(-)	0.86 (9)
MnO	1.5 (4)	1.5 (4)	1.5 (4)	2.0 (2)	1.58 (9)
ZnO	1.5 (4)	0.6 (2)	2.1 (6)	3 (2)	1.08 (9)
Cr_2O_3	0.25 (5)	0.6 (2)	(-)	1.0 (6)	(-)
Na_2O	2.6 (5)	1.4 (4)	(-)	5 (1)	1.4 (4)
Total	99 (5)	101 (4)	99 (4)	100 (4)	100 (5)
			mg kg^{-1}		
As	146	10	(-)	148	41
Cu	235	96	(-)	164	99
Hg	107	144	115	140	106
Mo	100	82	92	124	89
			Individual masses of aliquots of crystals/mg		
Aliquot 1	20.2	12.3	9.6	10.9	10.2
Aliquot 2	20.5	12.8	10.2	11.2	10.4
Aliquot 3	20.9	13.5	15.6	11.4	10.6

(-) means that any eventual presence of the element in the sample is in a content below the detection limit of the corresponding method of chemical analysis.

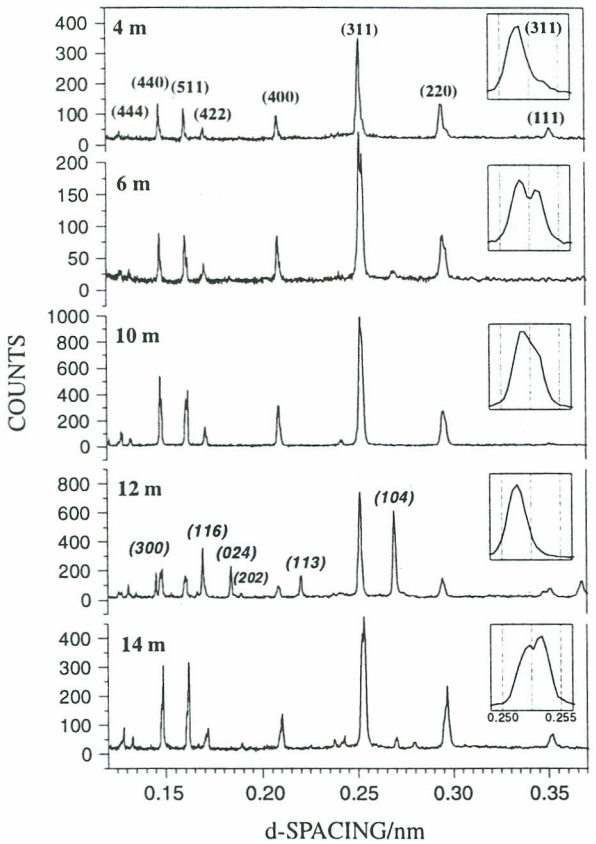

Figure 1. X-ray patterns of powdered crystals under analysis. Reflection planes of cubic iron-spinel are indicated for the 4 m sample and of the hematite for the 12 m sample (in italics). Inset: a magnified d-spacing scale view of the (311) reflection of the spinel phase is presented for each sample.

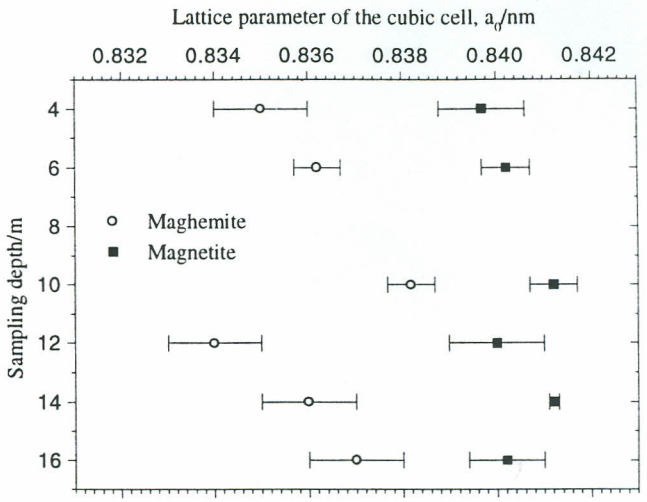

Figure 2. Lattice parameters of cubic cell of the iron-spinel. Two a-dimension values were determined in each sample, based on the split reflections of the powder X-ray patterns.

a_0-value of the cubic unit cell, corresponding to a (Mg, Ti)-rich magnetite, and the other with a_0 closer to the reported value for (Mg, Ti)-rich maghemite, by Fabris et al. (1995).

Only the higher a_0-value spinels (assigned to the magnetite precursor) of the present two groups is fairly (within 10% probability level) correlated (linear correlation coefficient, r = 0.73) with the sampling depth, taken from the top of the weathering mantle (see Figure 2, for a qualitative view).

The relative XRD intensities of the (311) split reflections in all samples vary asystematically: the 14 m sample has the component at highest $d_{(311)}$-spacing more intense than for all the other samples (insets, Figure 1). In the 4 and 12 m samples, only a peak asymmetry is actually observed. More intense XRD reflections due to hematite in the 12 m sample (Figure 1) are explained by the exsolution veins of anisotropic oxide in the iron spinel matrix, as can be seen on the optical micropetrographic image (Figure 3d).

Optical micropetrographical analysis

It indicates that hematite actually appears as an exsolution in the spinel matrix (Figure 3d). A complex pattern appears for sample 4 m (Figure 3a). Based on XRD data (Figure 1) most of the iron oxide spinel phase is maghemite, with a_0 = 0.835 nm. The 6 m sample (Figure 3b) shows two different patterns: one anisotropic zone assignable to ilmentite, with averaged composition from microprobe analysis (M = 152.36 g mol^{-1})

$$Fe^{2+}_{0.99}\ Ti^{4+}_{0.99}\ Mn^{2+}_{0.03}\ O_3 \qquad (1)$$

and one isotropic, for which the following nearly pure maghemite formula may be allocated (M = 211.96 g mol^{-1}):

$$Fe^{3+}_{2.63}\ Cr^{3+}_{0.01}\ Si^{4+}_{0.02}\ \otimes_{0.34}\ O_4 \qquad (2)$$

where $\otimes$ is a cation vacancy.

In two samples, collected at 10 m (Figure 3c), and 14 m (Figure 3e), more than one alteration zone is present (labeled A, B and C), with a clearly distinguishable homogeneous inner core and an altered outer layer, both isotropic under polarized light. A subtle intermediate zone appears in the 14 m crystals (Figure 3e); zone labelled B). Both samples are rich in Fe^{2+} (Table 1). The SEM probed crystal of the 10 m (Figure 3d) has a relatively large homogeneous core surrounded by a thin altered area. If all Fe^{2+} ions are assumed to be located in the core spinel, a more preserved phase, the microprobe analysis over the inner part of a polished section of a typical 10 m crystal (Figure 3) leads to the averaged formulae (3), M = 206.03 g mol^{-1} (the indexes, as in all formulae presently allocated, were

calculated from an average of elemental contents from determinations of three different points in the probed matrix):

$$Fe^{3+}_{1.55}\ Fe^{2+}_{0.48}\ Mg^{2+}_{0.38}\ Ti^{4+}_{0.35}\ Al^{3+}_{0.05}\ Si^{4+}_{0.01}\ Mn^{4+}_{0.01}\ \otimes_{0.16}\ O_4 \quad (3)$$

The external layer of this same sample has a composition corresponding to the formula of an assumed fully oxidized maghemite (M = 194.49 g mol^{-1}):

$$Fe^{3+}_{1.74}\ Mg^{2+}_{0.41}\ Ti^{4+}_{0.41}\ Al^{3+}_{0.08}\ Si^{4+}_{0.01}\ Mn^{4+}_{0.01}\ \otimes_{0.33}\ O_4 \quad (4)$$

Formula (4) is comparable to that of the (Mg, Ti)-rich maghemite identified from a high gradient magnetic separate from tuffite, by Fabris et al. (1995):

$$Fe^{3+}_{1.84}\ Mg^{2+}_{0.41}\ Ti^{4+}_{0.32}\ Al^{3+}_{0.07}\ Cr^{3+}_{0.03}\ Mn^{4+}_{0.02}\ Si^{4+}_{0.01}\ \otimes_{0.30}\ O_4 \quad (5)$$

with M = 196.88 g mol^{-1}.

The Fe^{2+}-rich spinel (3) corresponds to a highly (Mg, Ti)-substituted magnetite with the highest cubic unit cell dimension (a_0 = 0.8412 nm) and spontaneous magnetization (σ_s ~32 J T^{-1} kg^{-1}),

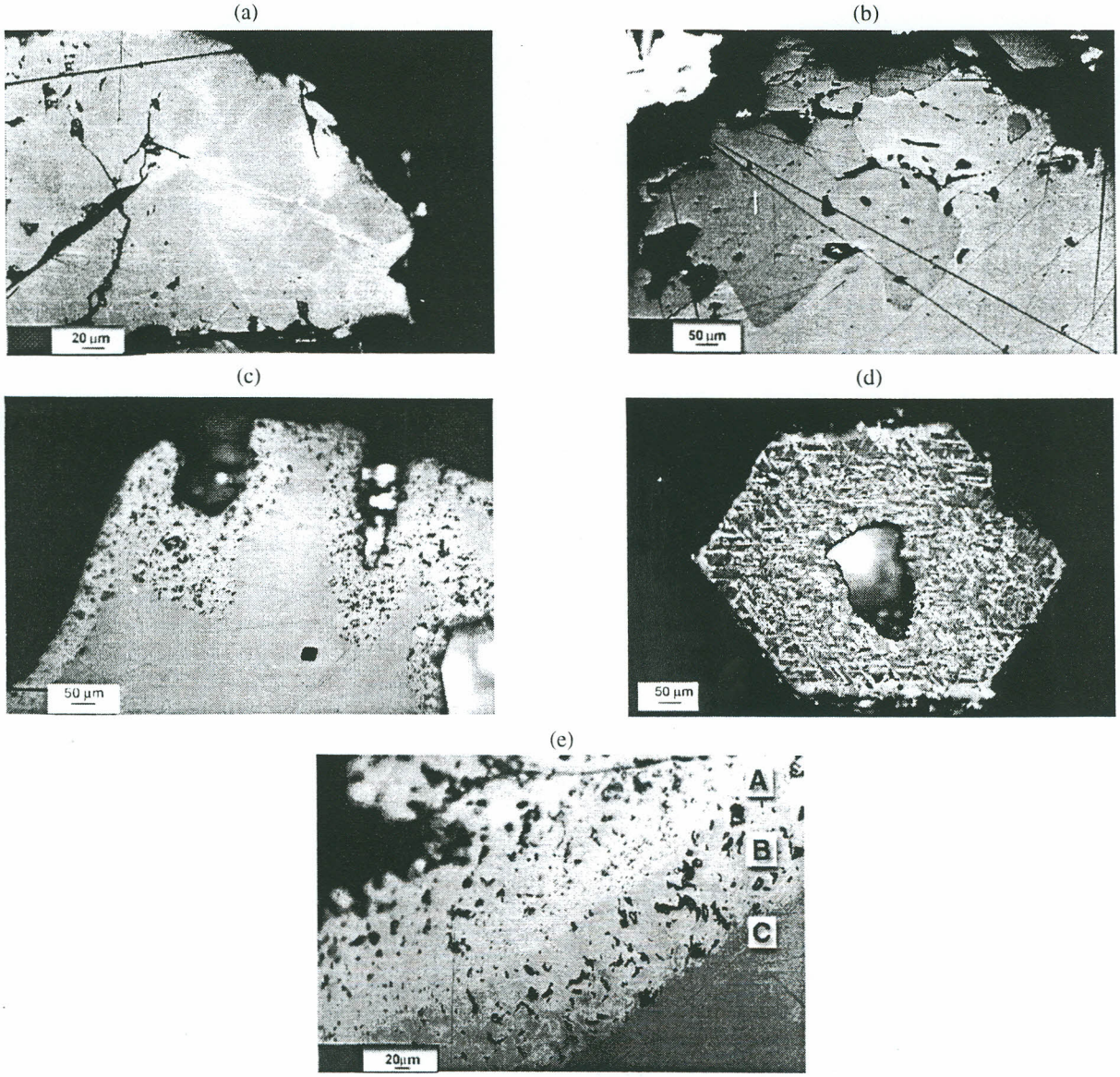

Figure 3. Optical micrographs, taken under a petrographical microscope with polarized light, of polished sections of crystals separated from samples collected from a tuffite mantle, at depths of (a) 4 m, with exsolution of hematite; (b) 6 m, with presence of ilmenite; (c) 10 m, with two alteration zones, an inner core and an oxidized external layer; (d) 12 m, presenting exsolution of hematite, along with inclusions of ilmenite and (e) 14 m, showing three alteration zones labeled A, B and C.

among all spinel phases being presently studied. This is very likely an igneous precursor of the (Mg, Ti)-rich maghemite of tuffite. These arguments are reinforced by optical micropetrographic analysis, that shows characteristic features of magnetite in the core and of maghemite in the outer layer (Figure 3c).

The existence of an intermediate alteration zone in the 14 m sample (Figure 3, labelled B) does not allow to unambiguously allocate all Fe^{2+}, determined by conventional chemical analysis of the set of crystals (Table 1), to the inner phase. If all iron is simply allocated as Fe^{3+} in this phase, the following formula is obtained (M = 197.89 g mol^{-1}):

$$Fe^{3+}_{1.90}\ Mg^{2+}_{0.36}\ Ti^{4+}_{0.33}\ Al^{3+}_{0.06}\ Si^{4+}_{0.01}\ Mn^{4+}_{0.01}\ \otimes_{0.32}\ O_4 \qquad (6)$$

With a similar approach, the compositions of the intermediate ((7), M = 197.77 g mol^{-1}) and the external layers ((8), M = 196.80 g mol^{-1}) correspond to:

$$Fe^{3+}_{1.88}\ Mg^{2+}_{0.33}\ Ti^{4+}_{0.36}\ Al^{3+}_{0.06}\ Si^{4+}_{0.01}\ Mn^{4+}_{0.01}\ \otimes_{0.34}\ O_4 \qquad (7)$$

and

$$Fe^{3+}_{1.85}\ Mg^{2+}_{0.31}\ Ti^{4+}_{0.39}\ Al^{3+}_{0.06}\ Si^{4+}_{0.01}\ Mn^{4+}_{0.01}\ \otimes_{0.36}\ O_4 \qquad (8)$$

The decreasing iron content (expressed in formulae (6) through (8) exclusively as Fe^{3+}) from the inner to the outer part of this crystal means that Fe (and also Mg^{2+}) is progressively lost from the lattice during the oxidation process, from the core to the external layer. The relative amount of Ti^{4+} increases in the same direction. The formula (6) is comparable to the core phase composition (9) reported by Goulart et al. (1997), for a spinel grain from a soil derived from tuffite of the same area, in which all iron content was allocated in its higher oxidation state (the numbers in brackets following the formula indexes were originally estimated uncertainties over the last significant digit, taken as standard deviations from the mean of corresponding probed points):

$$Fe^{3+}_{1.907(9)}\ Mg^{2+}_{0.388(4)}\ Ti^{4+}_{0.302(6)}\ Al^{3+}_{0.081(2)}\ Mn^{4+}_{0.011(1)}\ \otimes_{0.302(3)}\ O_4 \qquad (9)$$

Magnetization

Magnetization curves at room temperature (Figure 4) indicate an approach to saturation at a field of ~0.2 tesla in all samples, but spontaneous magnetization varies from σ_s ~8 J T^{-1} kg^{-1} (12 m) to σ_s ~32 J T^{-1} kg^{-1} (10 m). From chemical analysis (Table 1), these iron oxide samples are rich in structural (Ti, Mg) and contain some Al, which can help explain the lower σ_s-values relative to the pure maghemite (~60 J T^{-1} kg^{-1}) or magnetite (100 J T^{-1} kg^{-1}).

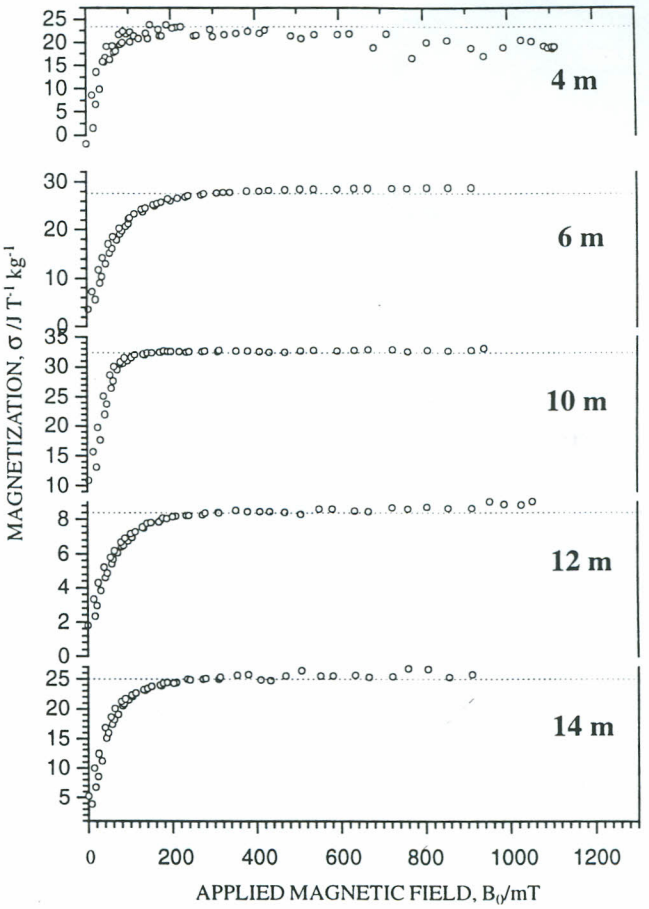

Figure 4. Magnetization measurement obtained from a selected single crystal of each sample group. Dotted straight lines represent linear reggressions comprising points of the plateau approaching saturation.

Isomorphical substituent Mg^{2+} ions reduced saturation magnetization as lattice incorporation. For instance, the saturation magnetization at 4.2 K, under an applied magnetic field of 5 tesla, in synthetically Mg-doped maghemites drops from 78 J T^{-1} kg^{-1} (pure, $Fe^{3+}_{2,67} \otimes_{0.33} O_4$) down to 25 J T^{-1} kg^{-1} $Fe^{3+}_{2,12} Mg^{2+}_{0.81} \otimes_{0.06} O_4$) (Mussel et al., 1997).

Magnetic susceptibility measurements

The magnetic behavior as a function of temperature is markedly different, from sample to sample. Magnetic susceptibility (expressed as voltage signal, Figure 5) of a crystal from the sample collected at 14 m exhibits a sharp increase at 131.8 K, which is due to the Verwey phase transition in magnetite. A comparative measurement of the magnetic susceptibility of a single crystal of a natural stoichiometric magnetite is also presented in Figure 5, for which T_V ~115.1 K. For all the other samples no such a clear transition can be observed.

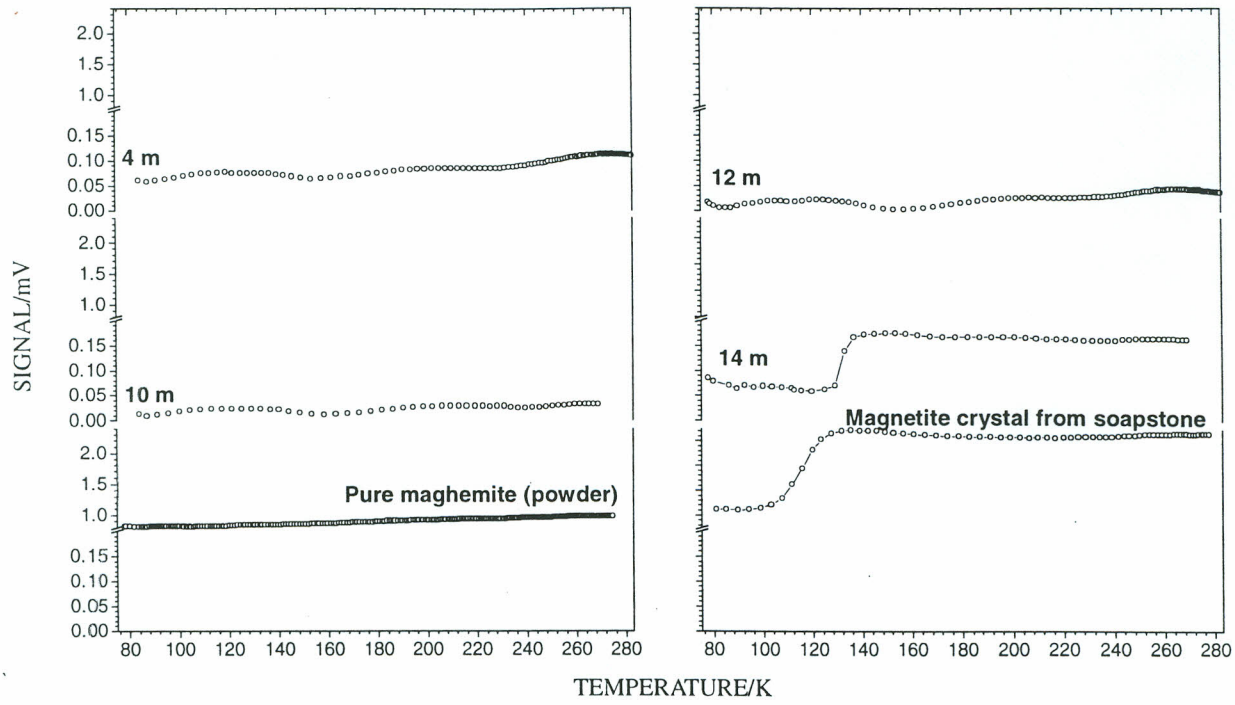

Figure 5. Magnetic susceptibility curves, expressed as electrical signal amplitude, of a selected single crystal of each sample. Pure synthetic maghemite (powder) and a crystal of magnetite from soapstone are also presented, for comparison.

Mössbauer

Mössbauer spectra of all samples, both at 298 K and 80 K are rather complex (Figure 6). Least-square fitting of these spectra requires a number of constrained parameters, which makes the numerical analysis somewhat artificial. Unless experimental refinements could be made, as by measuring with a strong (> 5 T) external magnetic field, no subspectral separation is unequivocally obtained. For this reason, the Mössbauer analysis here is qualitative. In spectra at 298 K, two features can be cited: the unequal intensities and widths of lines 1 (leftmost) and 6 (rightmost). For the 4 m sample, line 1 is more intense and narrower than line 6, whereas the inverse is observed for all other samples. In 10 m sample, line 1 presents an asymmetric shape with a right-side shoulder, suggesting that some high spin Fe^{2+} contributes to the total resonance absorption. From X-ray analysis, the Fe^{2+} would be very probably due to the presence of magnetite. This assignment was used by Fabris et al. (1997) to interpret the Mössbauer spectrum of these samples. In the 4 m sample, the spectral shape is more characteristic of Fe^{3+} in both sites of the dominant maghemite structure.

The Fe^{2+}-richer spinel phase is assumed to be the more preserved precursor of the (Mg, Ti)-rich maghemite, in the iron-rich phase assemblage. If so, the structural variabilities of the (Mg, Ti)-rich

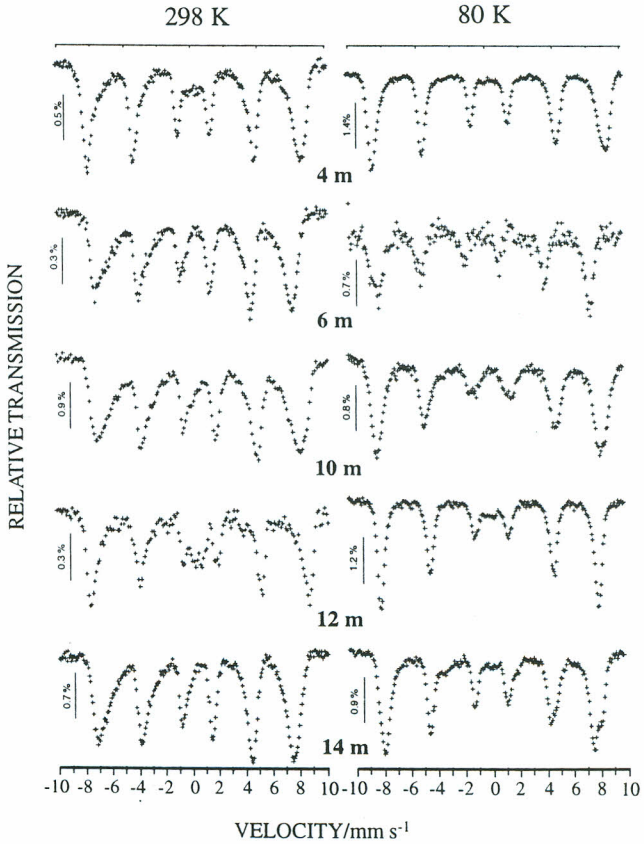

Figure 6. 298 K and 80 K Mössbauer spectra of powdered magnetic crystals.

maghemite is essentially related to the wide range of composition and cubic unit cell dimension of its precursor, (Mg, Ti)-rich magnetite, though the subsequent role played by fundamental weathering processes, involved in the Fe^{2+} oxidation during pedogenesis, can not be separately identified.

CONCLUSIONS

As far as the lattice parameter of the cubic cell (a_0) is concerned, two groups can be identified from XRD data: one of them with higher a_0-dimensions, ranging from 0.8397 to 0.8412 nm, and the other with lower a_0-values, from 0.834 to 0.838 nm. The first group can be related to an Fe^{2+}-richer spinel and is assumed to be the igneous precursor of the second, which has unit cell dimensions closer to that of (Mg,Ti)-rich maghemite. FeO contents from chemical analysis range up to 17 mass % and spontaneous magnetization σ_s = 8 to 32 J T^{-1} kg^{-1}. Zero-field room temperature Mössbauer spectra are rather complex, indicating that, the hyperfine field distributions due to Fe^{3+} and mixed valence $Fe^{3+/2+}$ overlap, producing very broad and asymmetric resonance lines. Only a qualitative Mössbauer analysis is actually provided, as the excessive number of parameter constrains, required to fit those spectra, gives very artificial results. The structural variabilities of the (Mg, Ti)-rich maghemite is assumed to be essentially related to the wide range of composition and cubic unit cell dimension of its precursor (Mg, Ti)-rich magnetite, though the subsequent role, played by fundamental weathering processes involved in the Fe^{2+} oxidation during pedogenesis on these variations, could not be safely separated and identified.

ACKNOWLEDGMENTS

Work financially supported by CNPq, FINEP and FAPEMIG (Brazil). CAPES (Brazil) granted a DSc fellowship to W.N. Mussel. We are indebted to Ms Kelen Cristina Lopes Martins (CNPMS/EMBRAPA, Brazil) for the technical support on the crystal separation and some chemical laboratory manipulations; to Ms Maria Beatriz Harmendari Vieira (Vale do Rio Doce Co., Brazil) for the optical microscope analysis and to Dr. Genilson P. Santana (Department of Chemistry, Federal University of Amazonas, Brazil) for some Mössbauer measurements.

To Dr. Derli P. Santana (CNPMS/EMBRAPA) and Professor Nilton Curi (Departamento de Ciências do Solo, UFLA) for their help on the soil sellection and soil sample collection.

LITERATURE CITED

CARMO, D.N.; CURI, N. & RESENDE, M. Caracterização e gênese de Latossolos da região do Alto Paranaíba (MG). R. Bras. Ci. Solo, 8:235-240, 1984.

CUGAT, O.; BYRNE, R.; McCAULEY, J. & COEY, J.M.D. A compact vibrating-sample magnetometer. Rev. Sci. Instrum., 65:3570-3573, 1994.

CURI, N. & FRANZMEIER, D.P. Toposequense of oxisols from the Central Plateau of Brazil. Soil Sci. Soc. Am. J., 48:341-346, 1984.

FABRIS, J.D.; COEY, J.M.D.; JESUS FILHO, M.F.; SANTANA, D.P.; GOULART, A.T.; FONTES, M.F. & CURI, N. Mineralogical analysis of a weathering mantle derived from tuffite. Hyperfine Interact., 91:751-757, 1994.

FABRIS, J.D.; COEY, J.M.D.; QI, Q. & MUSSEL, W.N. Characterization of Mg-rich maghemite from tuffite: Am. Mineral., 80:664-669, 1995.

FABRIS, J.D.; MUSSEL, W.N.; COEY, J.M.D.; JESUS FILHO, M.F. & GOULART, A.T. Mg-rich iron oxide spinels from tuffite. Hyperfine Interact., 110:33-40, 1997.

FERREIRA, S.A.D.; SANTANA, D.P.; FABRIS, J.D.; CURI, N.; NUNES FILHO, E. & COEY, J.M.D. Interrelações entre magnetização, elementos traços e litologia de duas seqüências de solos do estado de Minas Gerais. R. Bras. Ci. Solo, 18:167-174, 1994.

GOULART, A.T.; JESUS FILHO, M.F.; FABRIS, J.D. & COEY, J.M.D. Multiple iron-rich spinel phases and hematite of a magnetic soil developing on tuffite. Phys. Chem. Miner., 25:63-69, 1997.

JEFFERY, P.G. & HUTCHISON, D. Chemical methods of rock analysis. 3.ed. Oxford, Pergamon Press, 1981. 379p.

MUSSEL, W.W.; COLY, J.M.D. FABRIS, J.D. & JESUS FILHO, M.F. Mössbauer study of Mg-doped maghemite. Hyperfine Interactions, 2:53-60, 1997.